Scintillation in Argon Gas and Cosmogenic Simulations for NEXT-TON: a two-part study of event detection capabilities in neutrino experiments

Ryne S. Dingler [a] **and Benjamin J. P. Jones** [a]
E-mail: ryne.dingler@mavs.uta.edu , ben.jones@uta.edu
a. Department of Physics, University of Texas at Arlington
Arlington, TX, USA

ABSTRACT: Experimental neutrino physics is a field of constant technological advancement. Small-scale testing and simulations are essential for experimental development and adaptation. This study presents two experiments, one physical and one computational, in the interests of improvement event detection capabilities of gaseous media neutrino experiments. Our first experiment involves an analysis of the scintillation properties of gaseous argon. It has been shown that xenon-doped liquid argon is advantageous over pure argon due to its shorter time constant for radiative decay, which we hope to replicate using gaseous media. We have mad preliminary investigations of the potential experimental effects of environmental light, effects of organic fluor, tetraphenyl-butadiene, and application of electric field in pure argon.

In a separate study, we investigate a new tonne-scaled design concept for the neutrinoless double-beta decay experiments of NEXT. We present the results of cosmogenic neutron and muon event simulations to test improvements in background reduction for the latest experimental design. We find that the addition of a water tank shield around the detector reduces background neutron interaction to negligible levels, while the effects of muons events require further investigation.

Ryne Dingler X _____
ryne.dingler@mavs.uta.edu

Benjamin Jones X _____
ben.jones@uta.edu

1. BACKGROUND ON NEUTRINOS AND NEUTRINO DETECTORS

Mysterious and nearly impossible to detect, neutrinos are the second-most numerous known fundamental particles in the universe. They are electrically neutral leptons, fermions (spin $\frac{1}{2}$ particles) that only interact via weak-nuclear force and (hypothetically) gravity [1]. Each is coupled with a charged lepton, of the same flavor, as shown schematically in the cartoon image of the Standard Model (Figure 1). The three flavors of neutrino are electron, muon, and tau. Neutrinos have a small but non-zero mass, which displays different values of mass, contradictory to the original massless assumption in developing the Standard Model (Figure 1) [1].

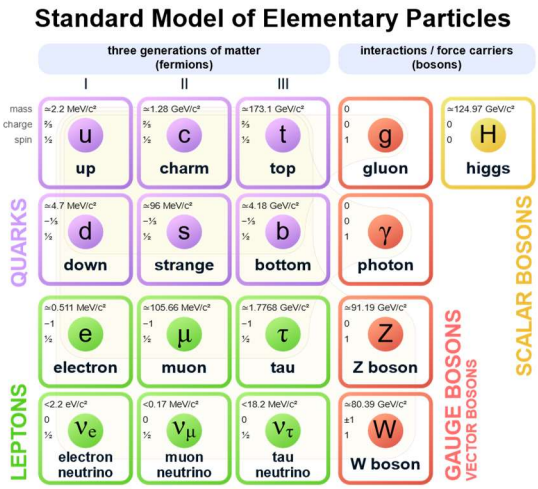

Figure 1. The Standard Model of Particles; neutrinos are seen on the lower most row of leptons in green [1].

Two major areas of research in neutrino physics are flavor-oscillations and the nature of antineutrinos. Neutrinos have the property that they exist in what is called a mixed state, wherein the flavor is well defined during creation and interaction but switching flavor and mass during oscillation [1]. This issue is a consequence of the probabilistic nature of quantum mechanics resulting in an indefinite mass due to mixing.

This project explores the questions of the neutrino's antiparticle. It was originally expected that neutrinos were Dirac particles meaning they had discrete antiparticles like the electron and positron. However, neutrinos violate charge-pair symmetry such that the mathematics to describe the physical state of neutrinos are not invariant upon mirror inversion as the other leptons [1]. This, combined with the fact that they have no conserved charges, allows for another possibility: that neutrinos are actually their own antiparticle, classified as Majorana particles. Theories suggest that a Majorana nature of neutrinos may explain the matter-antimatter asymmetry, leptogenesis, after the Big Bang which resulted to the matter dominated universe that now exists [1]. Experimental evidence of Majorana neutrinos would be the detection of a, yet to be observed, process called neutrinoless double-beta ($0\nu\beta\beta$) decay; this process will be further defined and explained ina following section. It is the goal of the Neutrino Experiment with Xenon TPCs (NEXT) to develop a detector with the ability to produce and observe $0\nu\beta\beta$ decay [2].

- ***DETECTION***

As stated, neutrinos are the second most common elementary particle. Millions of them are shooting through us all at any given moment, yet physicists count themselves lucky if they manage to see only a few. The difficulty in neutrino detection arises from their electric neutrality and solely weak-nuclear interactions. Consequently, neutrino detectors must typically be very large and underground to reduce environmental backgrounds. The detectors of particular interest in this study are scintillators; scintillation is further described in Section 1.2. Scintillators utilize the photoelectric effect in noble gas media (liquid or gas phase) to produce photons when valence electrons are excited or ionized by near passing or incident particles [2,3]. Media of choice for neutrino experiments are argon and xenon due to the readily available scintillation, ionization detection, energy resolution, and particle tracking capabilities [3,4]. In our experiment we will

investigate the scintillation properties of pure and xenon-doped argon gas, see Section 2. These results may prove useful for designs and development of future argon-based neutrino experiments [4]. In contrast, our computational study involves the simulation chamber of ^{136}Xe which is more conducive for 0νββ decay searches [1].

- **NEUTRINOLESS DOUBLE-BETA (0νββ) DECAY**

During beta decay, a neutron decays into a proton, electron, and an antineutrino. In an atom, this can be represented by the following equation,

$$ {}^{M}_{Z}X \rightarrow {}_{Z+1}{}^{M}X + e^{-} + \bar{\nu_e} \quad (1) $$

where X is the atomic symbol, Z is the atomic number, M is the atomic mass, e^{-} is an electron, and $\bar{\nu_e}$ is a neutrino. Double-beta decay is modeled similarly, but with two theorized possible outcomes given by,

$$ {}^{M}_{Z}X \rightarrow {}_{Z+2}{}^{M}X + 2e^{-} + 2\bar{\nu_e} \quad (2) $$

$$ {}^{M}_{Z}X \rightarrow {}_{Z+2}{}^{M}X + 2e^{-} \quad (3) $$

in which all symbols are the same as in Eq. 1. The two processes are illustrated in Figure 2. Normal double-beta (2νββ) decay is shown by Eq. 2, which is an observed phenomenon with a half-life of 1.1×10^{20} years [1]. Eq. 3 describes 0νββ decay which lacks neutrinos because, if neutrinos are their own antiparticles, those created have annihilated each other (Figure 2). This mode implies physics beyond the Standard Model (Figure 1) by violating lepton number conservation, in which the difference in lepton and antileptons is not conserved [1]. This process is predicted to have a

lifetime of ~10^{26} – 10^{27} years, or longer, but has never been observed [1]. Nevertheless, 0νββ decay is strongly supported by neutrino mass calculations and leptogenesis theories [1].

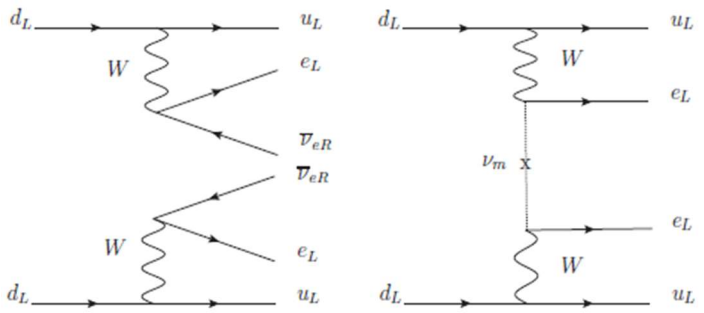

Figure 2. This figure illustrates Feynman diagrams for 2νββ (LEFT) and 0νββ (RIGHT) decay modes, including the virtual W bosons [1].

1.2 THE NEUTRINO EXPERIMENT WITH XENON TPCS (NEXT)

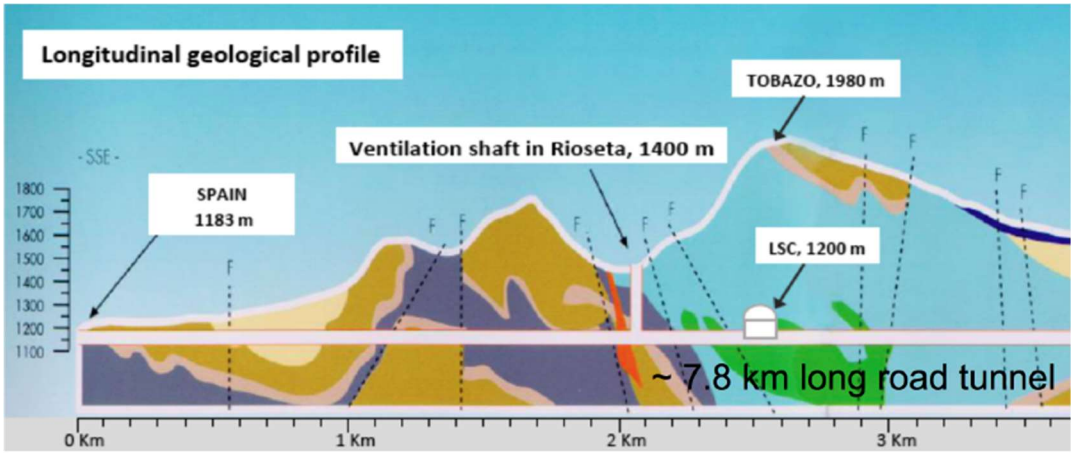

Figure 3. This image depicts the geological profile of the LSC and surrounding mountains [1].

The Neutrino Experiment with Xenon TPCs (NEXT) is an international collaboration of 13 Universities from 6 countries. It is experimentally based at the Laboritorio Subteranneo de Canfranc (LSC) in Canfranc, Spain. The experimental hall is located within the Tobazo mountain ~800 meters below the peak, providing natural radiation shielding (see Figure 3) [1]. They are faced with the daunting search of the elusive 0νββ decay. In order to successfully accomplish this task, the experiment design must continuously adapt and improve. It is currently in phase of

designing a tonne-scaled detection chamber, NEXT-TON. We thereby investigate the potential effects of background particles, particularly neutrons and muons, i.e. neutron captures, inelastic collisions, etc.

- ***VESSEL & DETECTOR***

NEXT-TON is TPC that utilizes 1000 kg of high-pressure ^{136}Xe as detection media. An electroluminescent region and scintillation allow for particle tracking over a photosensor plane [1]. The vessel cylindrically symmetrical measuring 162 cm in diameter, 324 cm long, and 2 cm thick with an inner copper shield that is 150 cm in diameter, 300 cm long, and 12 cm thick intended to reduce the vessels ^{208}Tl and ^{214}Bi radio-background [1]. There is also a surrounding water tank to reduce neutrons and gamma rays. Particle paths and energies are tracked using a Silicon Photomultiplier (SiPM) array that translates the light produce in ionization and deexcitation into a topological reconstruction. [1].

- ***SEARCH FOR 0νββ DECAY***

^{136}Xe undergoes ββ radiation and, though not common isotope, is relatively cheap to make and rarefy. Xe also has good particle tracking abilities as discussed in Section 2. All these factors make ^{136}Xe an ideal medium for 0νββ experiments. The goal of these experiments is to measure and analyze the energy of radiated electrons in ββ radiation to isolate a neutrinoless event. If successful, the sum of the electron energies will be commensurate with the difference in mass between the parent and daughter isotopes [1].

2. STUDIES OF SCINTILLATION IN ARGON GAS

While both gaseous and liquid media are used in neutrino experiments, gaseous particularly advantageous when either a low density medium or a strong energy resolution is required. Both of these are beneficial for searches for neutrinoless double beta decay, where energy measurement

allows to distinguish between the two- and no-neutrino modes. Studies of neutrino oscillations at short baselines in intense beams also benefit from low material densities to capture more information about the neutrino interaction events. On the other hand, at longer baselines where neutrino interactions are infrequent, denser liquid targets are required. Scintillation is a type of luminescence (light emission) that occurs when charged particles traverse a material. As particles travel through detector media, energy is transported through the electromagnetic fields to the gas. This energy then allows for either the excitation or ionization of electrons in the media, which releases light [3]. These processes are shown in more detail below by Figures 4, 5, and 6 We observe this light using a photomultiplier tube and oscilloscope. Light emission occurs from two spin-modes of excitation, a quickly occurring singlet-state and a slower triplet-state which will be the focus of our analysis, see Figure 4. We choose the longer microsecond scale triplet-state decay for this initial study because there is less potential error involved than the quick nanosecond scale singlet-state. Our study entails the collection of scintillation light produced by α radiation and measurement of the triplet-state decay time constants in pure and doped argon gas. This system is being calibrated with pure argon gas in order that future studies can test argon with added dopants that affect the scintillation timescale. However, we provide a description for how doped argon

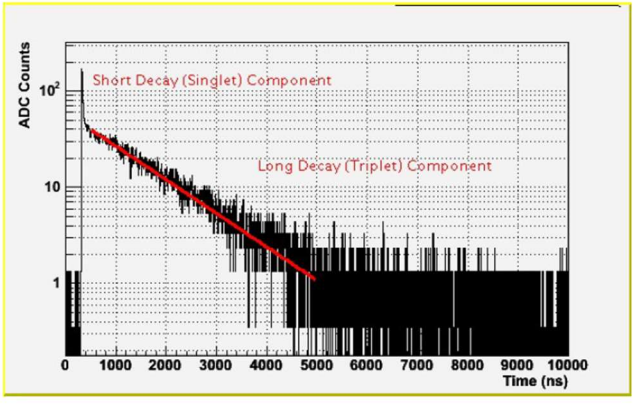

Figure 4. Above is a figure that demonstrates the singlet and triplet decays that comprise the signal from LAr [9].

scintillation should behave in hopes that we will soon move to this phase of the experiment. The details of scintillation in pure xenon are provided due to the relevance to our simulation of NEXT experiments though no pure Xe is used in our physical experiment. Further details of scintillation observation follow.

- ***PURE ARGON***

Argon in a popular medium for large scale particle detectors due to its high scintillation and ionization yields and lower cost than xenon [5]. In pure argon scintillation from triplet-sate deexcitation produces ultraviolet light at wavelength 128 ± 10 nm [5]. This radiative decay occurs with a time constant of ~3.1 ± 0.3 μs, though this time can be significantly truncated by the contamination of air [5,6]. Therefore, we must utilize a gas filtration system in our apparatus to minimize contamination. It may be possible that the scintillation may have a dependency on pressure. We therefore compare the resulting time constants against pressure (0-25 psig) to determine any possible relation.

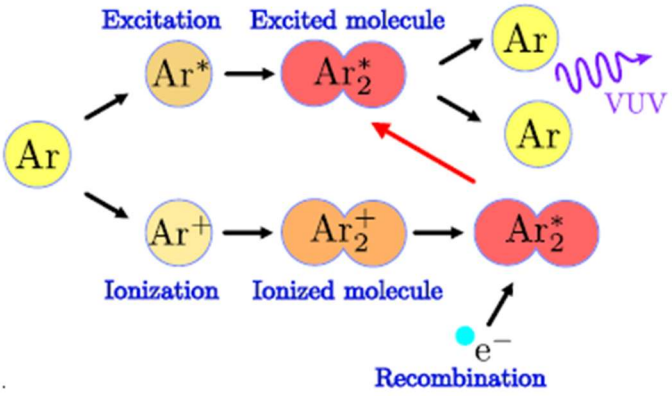

Figure 5. This figure illustrates the scintillation and ionization processes that occur in argon gas [5].

- ***PURE XENON***

Xenon gas is also a commonly used medium in neutrino experiments, particularly those interested in 0νββ decay because of its β-decay properties. Additionally, xenon yields advantageous energy

resolution and particle tracking qualities over argon [1, 7, 8]. Scintillation from the triplet-state excimer produces light at ~170 nm which is easier to observe than light from argon [8].

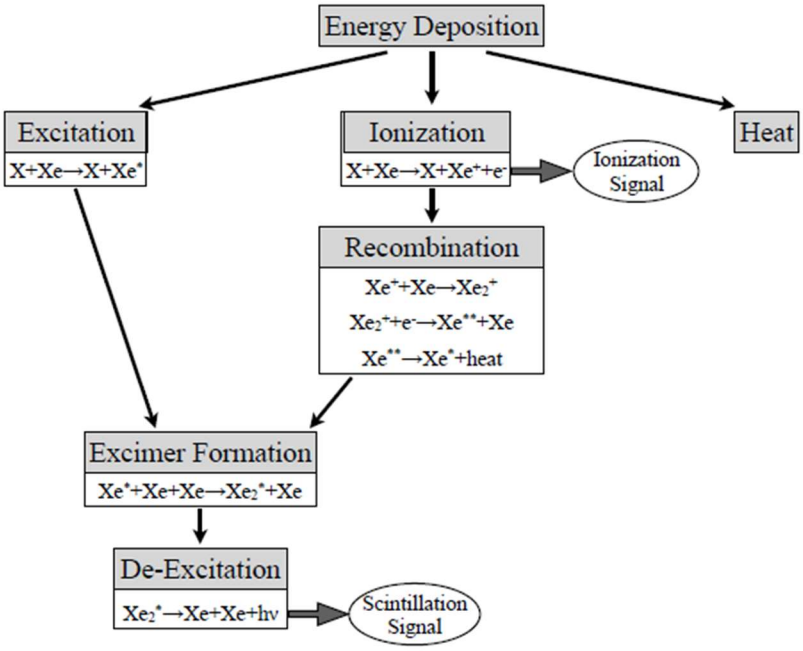

Figure 6. This flowchart depicts the scintillation and ionization processes that occur in xenon gas.

- ***ARGON – XENON MIXTURE***

Both argon and xenon hold their advantages in neutrino experiments. Xenon produces a better signal, but argon is more cost effective in large scale. Experiments using xenon-doped liquid argon (LAr) have shown that one can have the best of both worlds. Xenon valence electrons require less energy to be excited and therefore scintillate more readily than argon [9]. Ergo, scintillation from xenon-doped argon behaves more similarly to pure xenon even though the bulk of gas is argon [9]. Use of this type of media can increase efficacy for large argon-based detectors without a severe increase in cost.

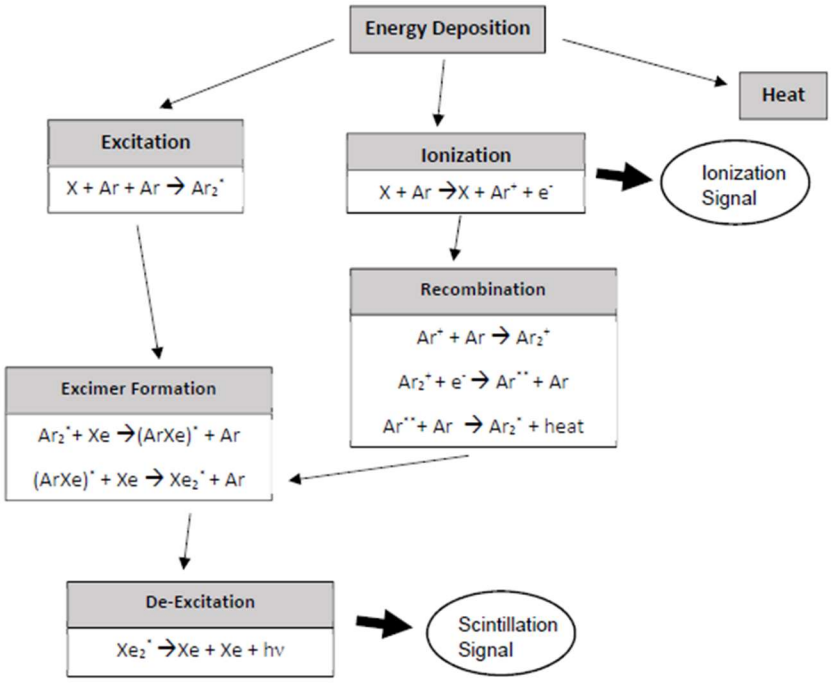

Figure 7. This flowchart depicts the scintillation and ionization processes that occur in xenon gas.

- **RESULTS IN LIQUID ARGON (LAr)**

As discussed previously, a doping of Xe in LAr has proven to effectively improve the quality of scintillation signal. It has also shown an increase in the efficiency of scintillation by reducing the time in which the excitation occurs as well as overall noise. The time constant for the triplet-state deexcitation in LAr of ~1.6 μs reduces to ~22 ns at concentrations 9 ± 5 ppm to 1100 ± 500 ppm xenon [9]. This notable improvement is demonstrated in Figure 7. This also provides for an increase signal yield from 4.0 ± 0.1 photoelectrons keV^{-1} to 5.0 ± 0.1 photoelectrons keV^{-1} [9]. Since gaseous detectors have shown to be better for these experiments, it is the goal of this experiment that similar results can be produced in doped argon gas in the interest of new gas-based detectors.

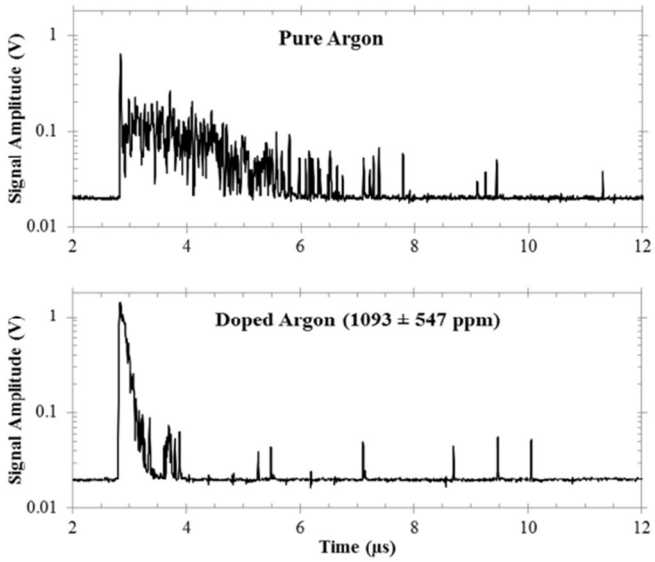

Figure 8. Above are figures that represent an observed signal in pure and doped LAr [9].

2.2 SCINTILLATION STUDY EXPERIMENTAL SETUP

- ***THE TEAPOT***

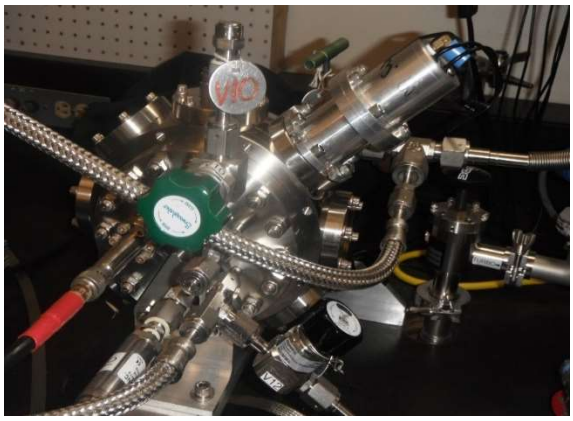

Figure 9. The TeaPot, located at the University of Texas at Arlington.

The TeaPot is a small scintillation and ionization chamber built at Lawrence Berkeley National Laboratory and repurposed for testing gas properties at the University of Texas at Arlington. Externally, the chamber measures 11.1 cm in width and 8.36 cm in diameter, not including the side flanges, and is capable of pressurization up to 8 bar [7]. Within the chamber are high voltage and signal electrodes with a gap of 5 mm, to create an electroluminescent region if necessary [7].

The signal electrode for is segmented with an inner 2.5 cm diameter section that is used to negate the effects of fringing from the two larger plates in topological analysis [7]. Part of this study will involve investigating the effects of an applied field. Though capable of housing up to 4 photomultiplier tubes (PMTs), see following section, we currently only use one for our observations. The PMT is negatively biased to -1250 V with an oscilloscope termination of 50 Ω, to provide for an optimal signal to noise ratio [7,10]. Additionally, to establish the best possible conditions, we test the effects of environmental light and the addition of a wavelength shifting compound tetraphenyl-butadiene (TPB). TPB has been shown to absorb the UV radiation and remit it at a visible and 430 nm and so will help ensure radiation is unimpeded by the observation windows if necessary.

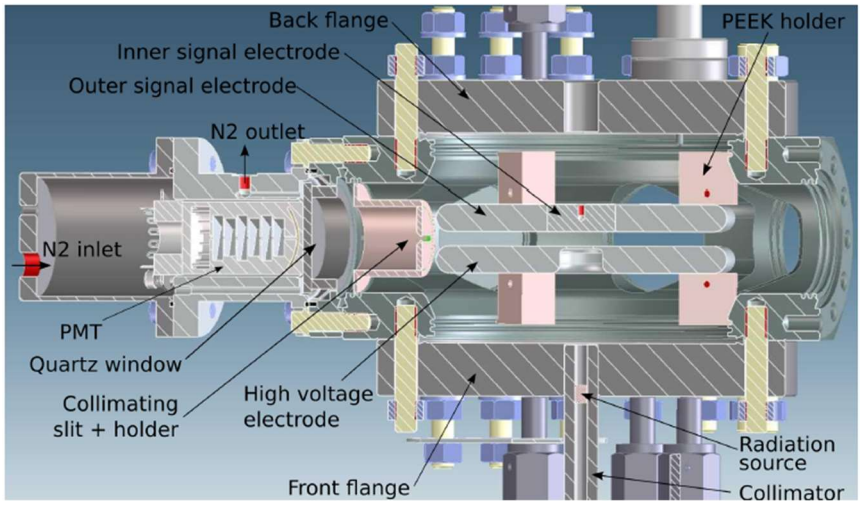

Figure 10. The above figure illustrates the internal schematic of the Teapot with an attached PMT [7].

- ***PHOTOMULTIPLIER TUBES (PMTs)***

Photomultiplier tubes are devices that allow for the amplification of small photon emissions by generation of a photoelectron cascade. Light enters the tube where it is incident upon a photoelectrode which releases excited photoelectrons into the internal vacuum. These photoelectrons then ricochet through a series of dynodes that continuously generate more

photoelectrons [10]. This amplification process can translate a single photon to an observable signal on the scale of millions of photoelectrons [10]. This process is illustrated in Figure 10. Though many electrons comprise the observed signal, the small charge of an electron means that we observe a relatively small drop in potential below the noise threshold, defined by us a pulse. Further description of what defines a signal or pulse in our experiment can be found below.

- **DATA COLLECTION**

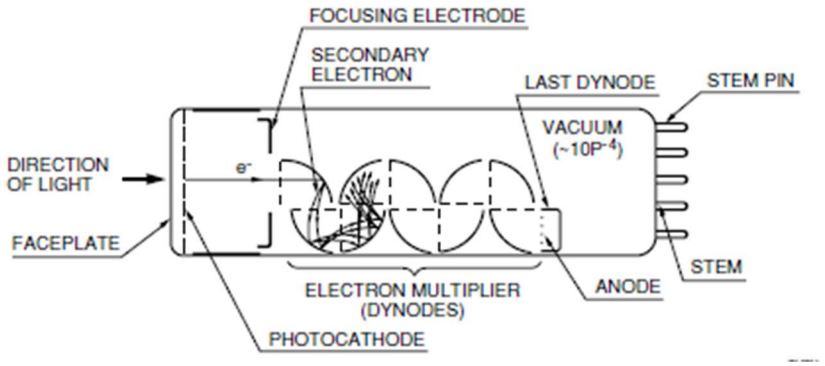

Figure 11. This image illustrates how a PMT generates a signal by a photoelectron cascade [10].

The Teapot can be pressurized up to 8 bar or 116 psig, though initial testing is set between 0-25 psig [7]. The chamber and all tubing must first be evacuated to a vacuum pressure $\lesssim 10^{-8}$ bar. The gas is then filled through a filter and cold getter, flushed, and refilled to help avoid contamination. For this experiment, we examine the scintillation produced by α-radiation from ^{210}Po. We observe ~10000 signal pulses per sample, as described above. We define a pulse as a point in the waveform where the signal drops below a trigger threshold, set as -5 mV, above the noise level. These waveforms are saved as binary files which are translated and synthesized into usable data which can be used to develop average waveforms and analyze radiative decay properties from normalized pulse histograms as described in the following section. Data is to be normalized by the pulse frequency, but the oscilloscope used to measure these rapidly occurring waveforms is limited by

how fast it can collect and save. Therefore, to distinguish a proper frequency of scintillation, we have connected the system to an octal discriminator and scaler counter. Frequency is calculated by collecting X number of waves within two minutes and dividing by 120 for a measurement in Hz.

- **ANALYSIS METHOD**

Analysis of data is done by use of standard Python packages and data reduction techniques. To analyze the radiative properties, particularly to determine the time constant for radiative decay, of the gas, we must take count of how many pulses occur over our observed time range. We thereby develop histograms to track these pulse counts by searching through each point in time in each individual waveform. If the waveform has surpassed the designated trigger threshold at that point in time, we consider a pulse to have occurred which is recorded in our histogram. It is observed that the number of occurring pulses decreases at an exponential rate; therefore, we base our analysis on the law of exponential decay as shown in Eq. 4. Analyzing the histograms in a logarithmic scale linearizing the exponential segments of our waveforms such that Eq. 4 becomes Eq. 5.

$$N(t) = N_0 e^{-kt} \tag{4}$$

$$\ln|N(t)| - \ln|N_0| = -kt \tag{5}$$

A linear fit is then generated over the late, slow end of the pulse as it decreases back to the baseline using Numpy's polyfit function. By utilizing the relation $\tau = \frac{1}{k}$, the time constant can then be taken as the negative-inverse of the fit's slope.

2.3 PRELIMINARY RESULTS FOR SCINTILLATION STUDY

We continue to test our results across pressures 0-25 psig; however, we must further constrain our setup to provide a viable control in pure argon prior to testing with xenon doping. For this reason, we present our progress in developing an optimal experimental setup at 0 psig and vacuum with

one series of time constant measurements across our pressure range. We first establish the signal produced by our radiation source in comparison to the signal produced by natural factors such as cosmic rays or radio-impurities in the chamber. We also compare scintillation in vacuum and pure argon pressurized to 0 psig. Data for such comparison is normalized by dividing by the integration of the pulse histogram and multiplying by the pulse rate. Normalization by pulse rate creates a direct proportionality between the pulse yield and rate. We also convey the effects of environmental light and the addition of TPB to our chamber.

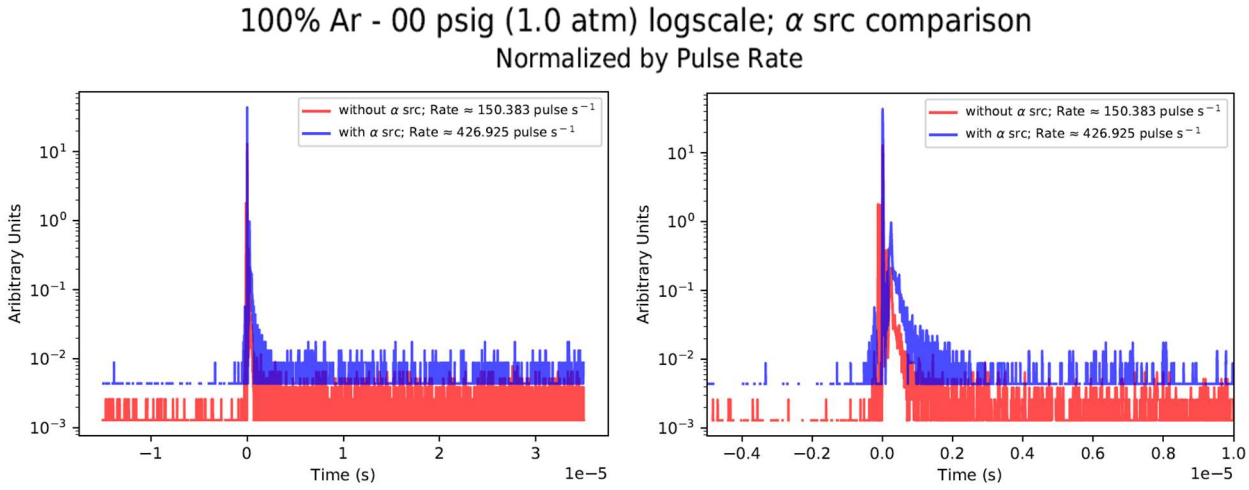

Figure 12. The plots above displays of the scintillation yields with and without the alpha source normalized by the pulse frequencies of ≈ 426 Hz and ≈ 150 Hz, respectively.

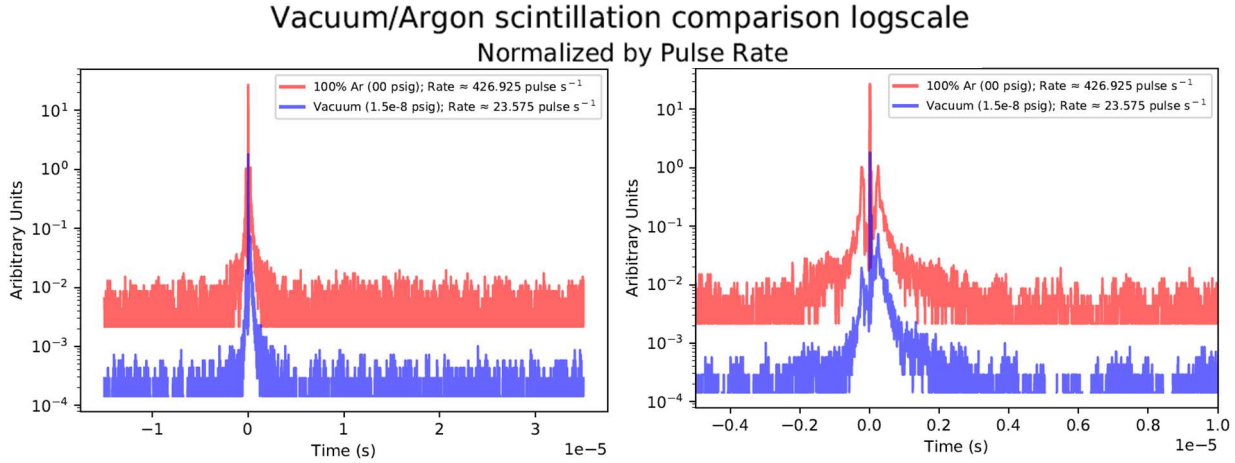

Figure 13. Normalized histograms to represent a comparison of the radiative decay in pure argon gas at atmospheric pressure and vacuum.

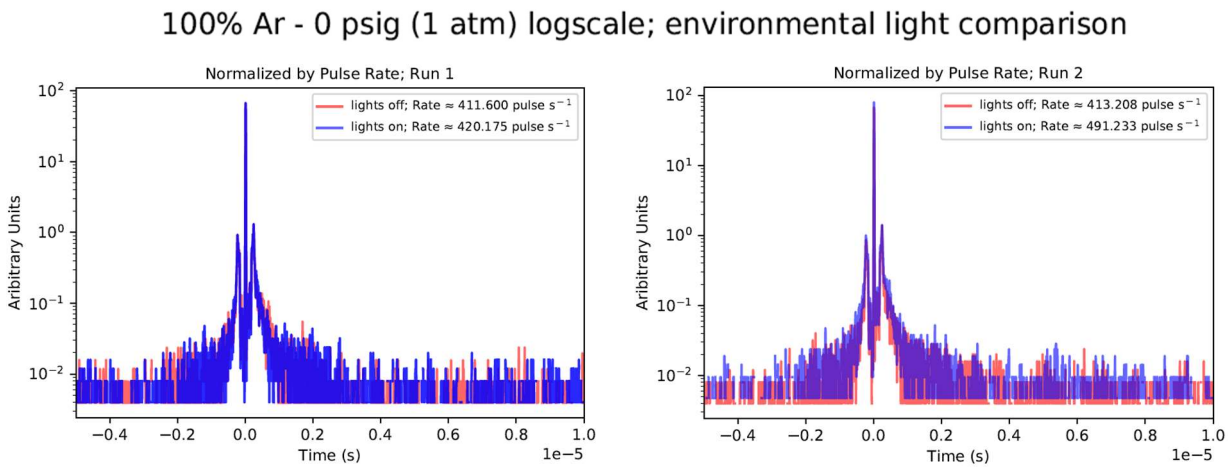

Figure 14. Normalized histograms to represent a comparison of the effects of environmental light on the radiative decay in pure argon gas at atmospheric pressure.

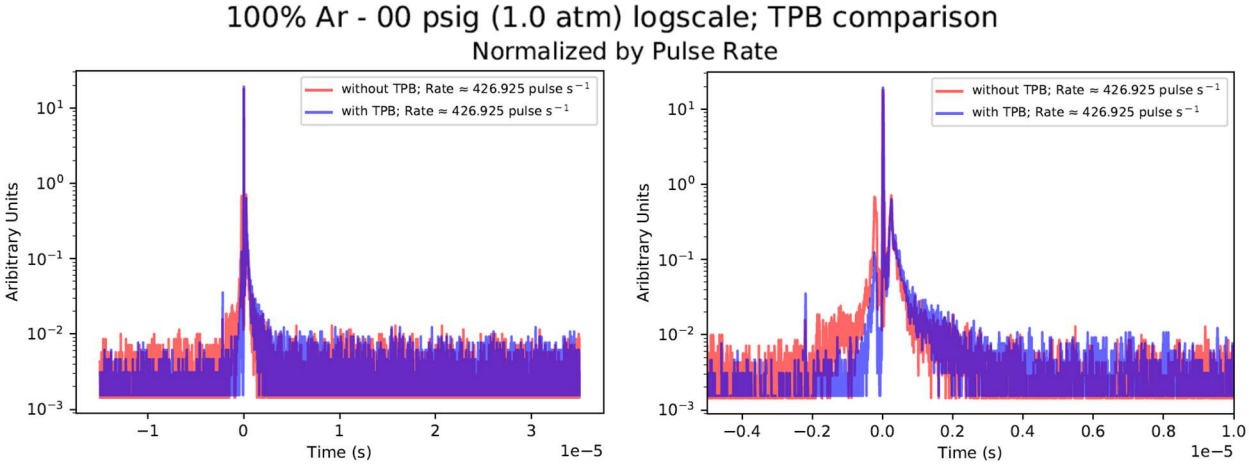

Figure 15. Normalized histograms to represent a comparison of the effects of tetraphenyl-butadiene on the radiative decay in pure argon gas at atmospheric pressure.

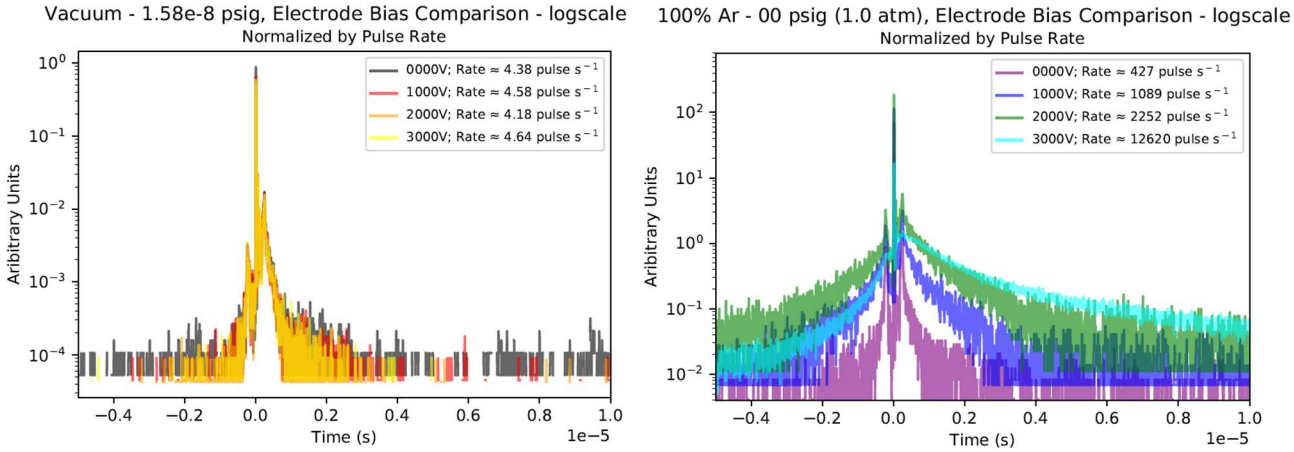

Figure 16. Normalized histograms to represent a comparison of the effects of applying a high voltage bias to the internal electrodes in vacuum (LEFT) and pure argon (RIGHT).

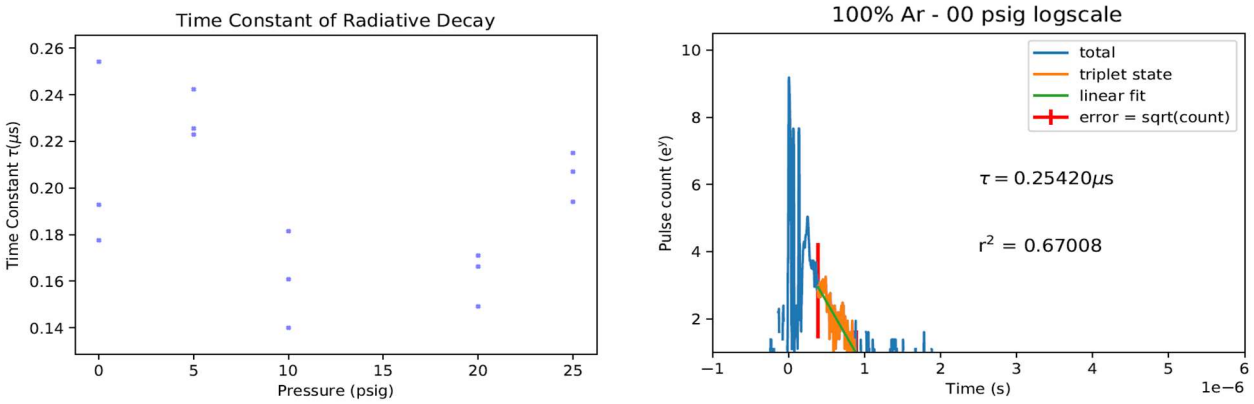

Figure 17. The figure above on the left displays an initial comparison of time-constants for expected pressure-dependence. The figure to the right provides an example of how noise-reduced histograms are fit to provide the time constant.

2.4 DISCUSSION OF SCINTILLATION STUDY

It is important that we distinguish between the scintillation signal produced by our radiation source and that caused by natural phenomena like cosmic rays. Hence, we compare our pulse signals with and without ^{210}Po. It is shown in Figure 12 that the normalized scintillation yield and pulse frequency are ≈ 183.89% greater by normalized integration with the inclusion of an α-radiation source. It may prove useful later to subtract the levels of scintillation that would occur without the source to isolate effects solely by α-radiation.

Figure 13 demonstrates that the light-yield and pulse rate are significantly greater by ≈ 1711% in argon gas than that in vacuum. This provides verification that scintillation is occurring in our media. Again, we may later find it advantageous to subtract the levels of scintillation that would occur in vacuum to isolate effects solely by the gas. These are expected results; nonetheless, we have demonstrated that they are the case for our experiment.

Light contamination poses a threat to our experiment considering the extreme sensitivity of our photomultiplier tube. Any extra light in the chamber can yield falsely high scintillation counts and truncate the time constant measurement. Our chamber is designed to prevent light from

entering by covering any window with a PMT which has a front-end rubber gasket which should seal any edges. For this reason, testing was originally done with the room lights on under the unsafe assumption that it would not affect our results. However, we found it prudent to test and confirm this assumption. Figure 14 shows that tests with the lights on provides for a somewhat higher pulse yield and frequency by ≈ 11.54% by normalized integration. While the increases are not severe, we thereby find that it would be best practice to do any further testing without extra lights on in the room.

If scintillation light is impeded or absorbed by the windows of either the PMT or with TeaPot, the pulse yield will be less, and the decay will be shortened. The addition to TPB may aid in preventing any loss of light by shifting the UV emission to more easily observed visible light. Figure 15 demonstrates this comparison. Addition of TPB to our chamber incorporates further difficulties. Our TPB is applied to thin sheets of metallic foil which must be placed between our source and PMT. With only a 5mm gap in this region, our options are to either stick the foil to the electrodes or carefully suspend the sheets by non-conductive wire. For simplicity in initial testing, we have chosen to apply the foil the to the electrodes; however, the conductivity of the foil means that a field cannot be applied to this configuration. We find the that addition of TPB in our experiment has shown no significant difference in yield or pulse frequency. This result is not well understood and is the subject of further study.

Application of an electric field may prove beneficial by amplifying the scintillation signal with electroluminescence. By biasing our internal electrodes this field can be generated. We have yet to constrain our electroluminescent region. However, we have established that our electrodes can be biased as high as 8000V in vacuum and 3000V at atmospheric pressure. That fact that voltage above 3000V cannot be applied is possibly due to Paschen's law in which an electrical arc

is created across the plates and effectively shorts our system. This may be also due to the buildup of electric charge on internal insulators like the PEEK holders. Neither of these predictions have yet been confirmed though we are examining this issue. While we observe no significant change in scintillation in vacuum due to our field, there does appear to be significant improvement in yield when the chamber is pressurized. We find a 155% increase in yield when our electrodes are biased to 1000V, a 499% increase at 2000V, and a 2855% increase at 3000V. This has shown the greatest effect on our system and is likely key to achieving our intended result. A cursory check of the resultant time constants of these waveforms (not included) has shown that a bias of 2000V still has a short time constant while 3000V create a time constant that is long. This mean we may be able to find a, "sweet-spot," between 2000 and 3000 volts that provides the correct amount of electroluminescence for our experiment.

It is believed that at higher pressures, the time constant of decay may be shorter due to the density of the medium. We therefore compare a series of initial time constant measurements at various pressure to test this hypothesis (see Figure 17). Time constants are calculated as described in our analysis section. These time constants, as well as those for all testing scenarios thus far, are unexpectedly short and may not be representative of the actual value. At this time, we see no dependence on pressure; however, this result will be continuously reexamined as we further develop or experimental conditions. Additionally, these values were collected by analysis of waveforms before normalization. Continuing analysis will be done using normalized histograms.

3. STUDIES OF COSMOGENIC BACKGROUNDS IN NEXT

Any neutrino experiment is faced with the difficulty of reducing natural backgrounds. Those that may provide false signatures of $0\nu\beta\beta$ can be interactions with radon, muons, neutrons and some natural radioactivities [1,11]. Estimates show a background flux for the NEXT-TON design at 2.59

$\times 10^{-6}$ counts keV^{-1} kg^{-1} yr^{-1} from muons and the copper shielding [1]. We investigate further the background effects of these cosmogenic particle interactions through simulation in potential experimental design configurations. This simulation process is explained in greater detail in in a following section.

- ***NEUTRONS***

Neutrons can be created by radioactivity in laboratory rocks or in the upper atmosphere by cosmic rays [1, 11]. Neutrons from cosmic radiation are highly energetic and easily permeate materials. Scattering from light nuclei and neutron capture processes induce background radioactivity and gamma radiation [11]. Luckily, neutrons can be easily accounted for and vetoed in experiments by data reduction techniques or shielding by molecules with high propensity for neutron capture [11]. The total neutron flux through the experimental hall of the LSC has been measured at $\Phi \approx 1.38 \times 10^{-5} \pm 0.14$ counts cm^{-2} s^{-1}, ranging in energy from $\sim 1 \times 10^{-10}$ – 100 MeV [1]. A neutron capture by ^{136}Xe forms ^{137}Xe which is a β-decay source. The resultant radiation emulates the desired signal proving troublesome for distinguishing a true $0\nu\beta\beta$ event [1,11]. Previous experiment design prototypes and simulations yielded impermissible levels of background caused by neutrons with ^{137}Xe activations >2.4 MeV within the first 5 milliseconds. [1]. The latest design incorporates an encompassing water tank rather than previous polyethylene shields [1]. It is thereby our responsibility to simulate this configuration and analyze the resultant nuclear interactions with detector in expectation that we will see an improvement from previous models.

- ***MUONS***

Along with neutrons, muons are also highly energetic particles, created in the upper atmosphere by cosmic radiation. They compose a majority of energetic particles near the ground and precipitate over half of the background associated with ^{137}Xe activation [1,13]. About a ninth the

mass of a neutron, they travel with much higher energy - about 220 GeV on average through the LSC [1]. Muons interact in various manners, i.e. scattering, nuclear captures, nuclear cascades, and secondary neutron production, which makes them more difficult to reduce than neutrons [1,12]. The neutrons generated by muon-interactions can then create ^{137}Xe providing the same issue as discussed in the previous section. Muons are overall easy to track via tagging and topological reconstruction; however, this process does not reduce the contributions by ^{137}Xe activation due to its long lifetime [1]. Therefore, we must proceed with the simulation of cosmogenic muons to determine the potential for creation of ^{137}Xe and other radioactive isotopes.

3.2 SIMULATIONS AND SOFTWARE

- ***GEANT4***

GEANT4 is an object-oriented toolkit, written in C++, for the purposes of nuclear and particle physics. It can produce physical models of particle interaction across a wide energetic and electromagnetic range based off user specified configurations and applicable physics [13]. The object-oriented nature of this GEANT4 allows for the generation of tailored scenarios in a global structure based on bottom-up dependencies [13]. This allows for open user design, visualization, and interfaces with the specified simulation [13]. A more detailed description of this process is provided in the following section regarding NEXUS.

- ***NEXUS***

NEXUS is a program that utilizes specialized features of the GEANT4 toolkit to Monte Carlo simulations of particles for an assortment of NEXT detector configurations. Initially, the user must develop macro files that specify the detector geometry and components, physics packages, and the energy and quantity of events/particles generated [1]. These factors are then called and

implemented in the simulation. The results are then saved into an output file which must be analyzed using external methods. This general process is illustrated below in Figure 18.

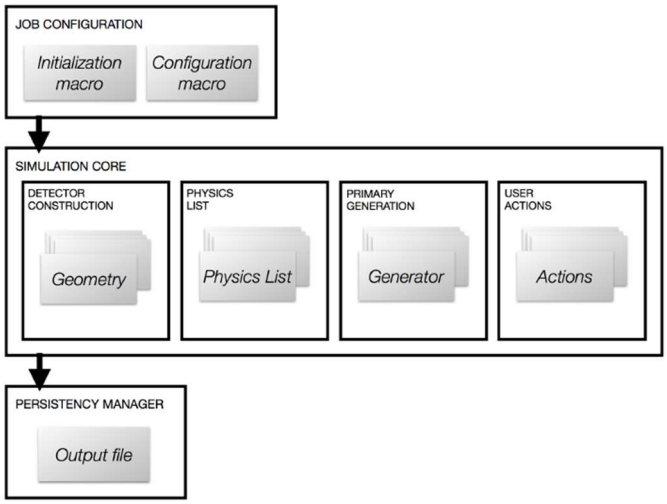

Figure 18. This diagram illustrates the general behavior of the NEXUS program via the GEANT4 structure [1].

To elaborate, particles or events of limited random momentum and position are produced via a generator which induces a detector response. These events are then reduced to those that fit the prescribed simulation criterion. After tracking the particle, the energy deposition and photosensory information is then recorded as a hit and translated to data structures or digits. During this phase,

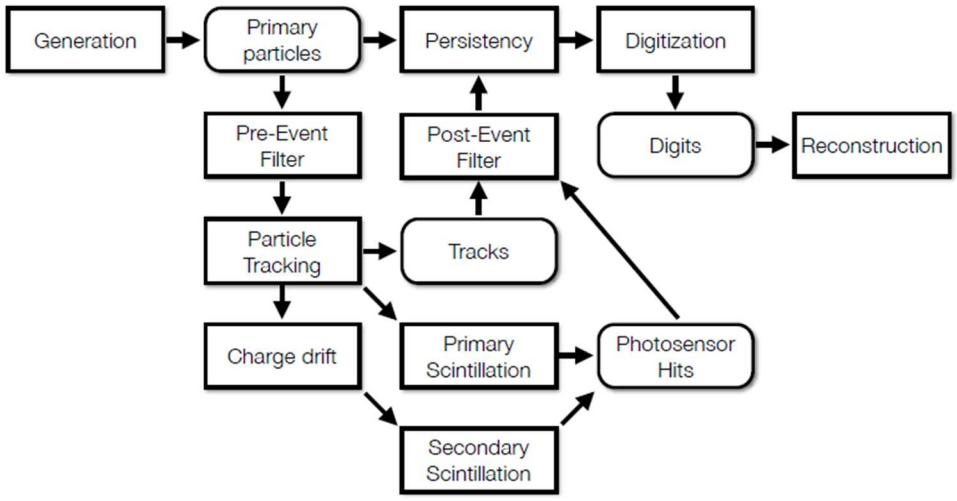

Figure 19. The flowchart above depicts the flow of data with a NEXUS simulation, where rectangular boxes indicate computations and rounded boxes indicate data sets [1].

noise is introduced which must be removed before information is stored. This is visualized by the flowchart provided in Figure 19.

- **SIMULATION**

In this study we generate Monte Carlo simulations of neutron and muon events on the order of millions of events. The particles originate from a virtual surface outside the detector. These events are designated at realistic energies determined from measured occurrences as discussed above [1,11,12]. For purposes of testing background contributions, we implement what is deemed a fast simulation in which scintillation and ionization signals are neglected [1]. This method of simulation is validated by extensive testing and comparison to fully parameterized simulation. By using this method, we allow for valid pseudo-reconstruction of event data without the need for heavily computational burden. Due to the overall low likelihood of neutron interaction in the detector, events must be generated on the scale of millions of events. Adequate statistics were achieved for neutron generation by generation of 4 million events per simulation.

- **ANALYSIS METHOD**

Data is analyzed by generation of an interaction history between event particles and detector molecules by assigning each atom or molecule a numbered designation. This history can then be used to follow then generated events through their interactions, deposited energy, and creation of daughter isotopes. The interactions of importance in our study are neutron captures due to the high potential for ^{137}Xe activation. Besides ^{137}Xe, we also keep track of the activation of ^{64}Cu, ^{66}Cu, ^{116}In, and deuteron which are also expected products of neutron capture. All other neutron capture processes are labeled as other. These isotopes counts are then normalized by the detector cross sectional area and the total flux of neutrons ($\Phi \approx 1.38 \times 10^{-5}$ cm^{-2} s^{-1}) through the LSC to provide the expected count per year. We also create histograms for the deposited energy as well the time

for radioactive decay in ^{64}Cu, ^{66}Cu, and ^{137}Xe to determine the implications on the experiment if these daughter isotopes are created.

3.3 RESULTS FOR COSMOGENIC SIMULATIONS

- **NEUTRON GENERATION**

In this section we present the results of our neutron event simulations for the NEXT tonne-scale design. The figures below show the results from the generation of 4 million neutrons at energies 40-100 MeV. Events were also generated in samples of 1 and 2 million; however, they do not produce results statistically significant enough for this experiment. Neutrons generated below 40 MeV demonstrate no significant isotopic production or interaction within the detector. Therefore, results for simulations below 4 million events 40 MeV are omitted. It should be noted that not all neutron capture processes involve the exterior neutrons but may be a consequence of secondary neutron creation within the detector.

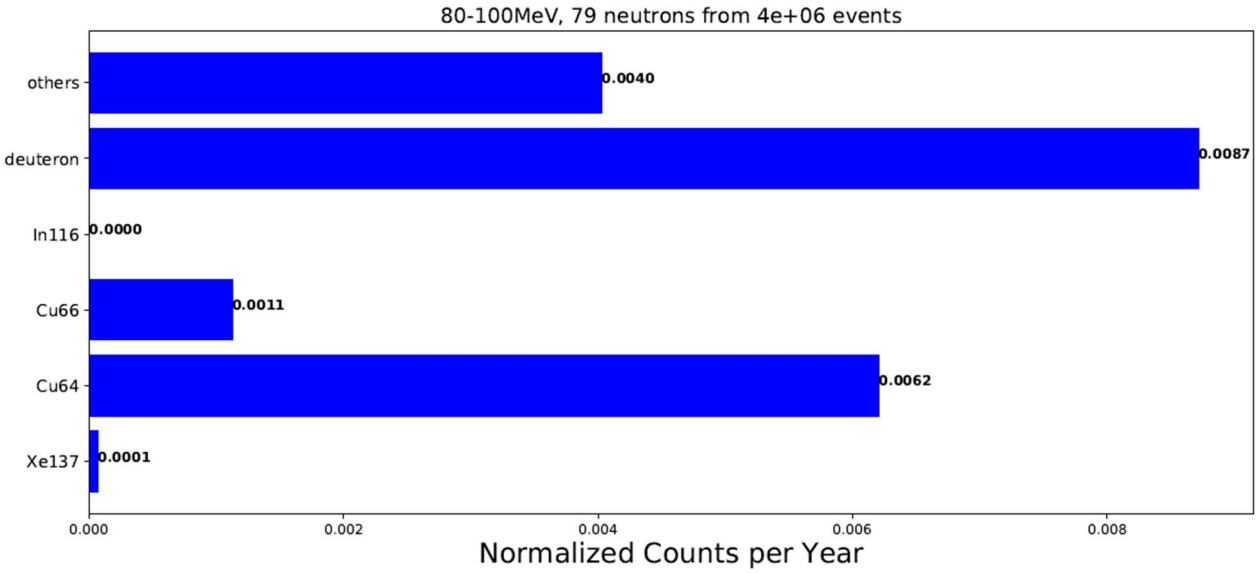

Figure 20. The figure above displays the normalized counts of isotopes of interest within the detector. These are resultant from 79 neutron captures out of 4 neutrons million generated at 80-100 MeV.

Figure 20 shows the creation of one ^{64}Cu isotope per 161 years, one ^{66}Cu per 909 years, and one ^{137}Xe per 10,000 years due to cosmogenic neutrons. Associated energy deposits and decay times are shown below in Figures 21-23.

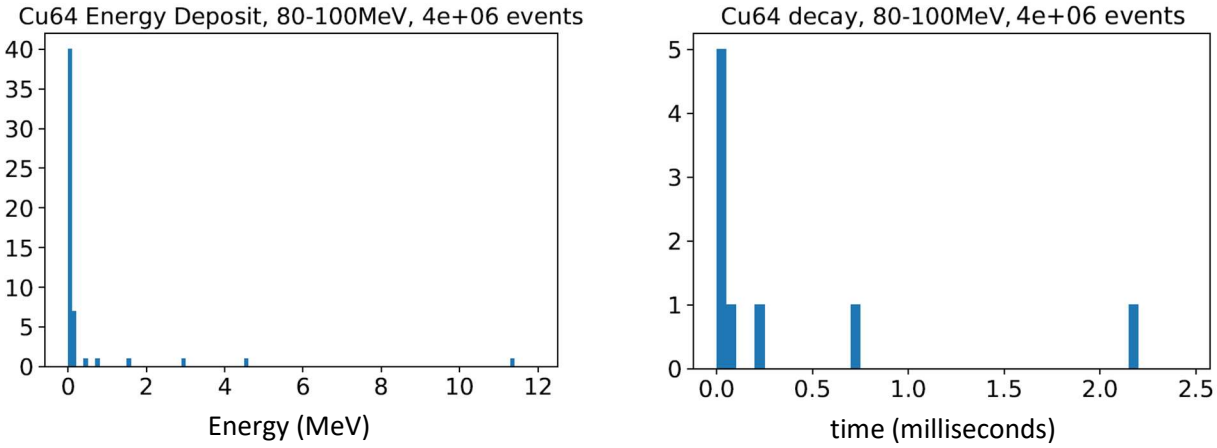

Figure 21. The above histograms display the deposited energies (LEFT) and the time for radioactive decay (RIGHT) for created ^{64}Cu for events at 80-100 MeV.

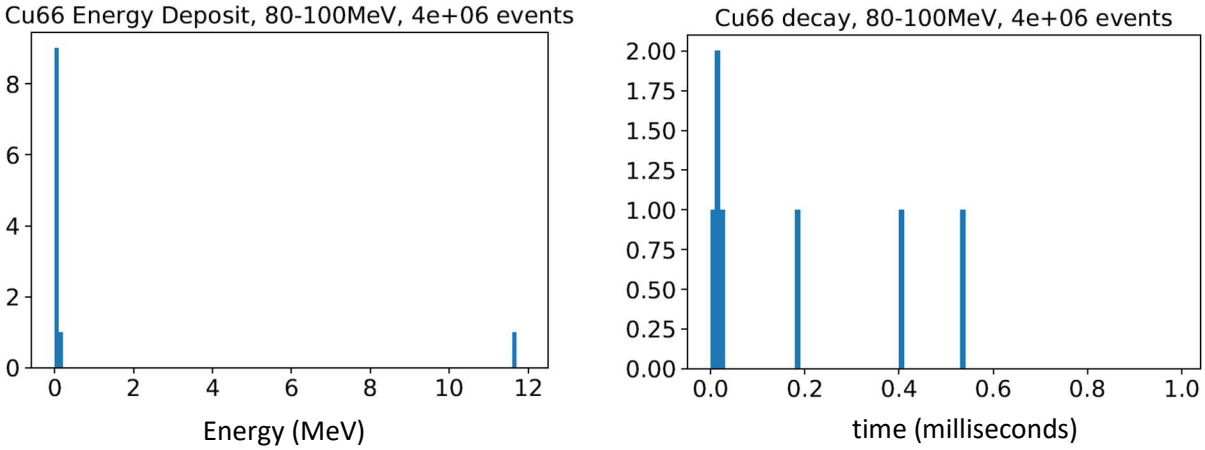

Figure 22. The above histograms display the deposited energies (LEFT) and the time for radioactive decay (RIGHT) for created ^{66}Cu for events at 80-100 MeV.

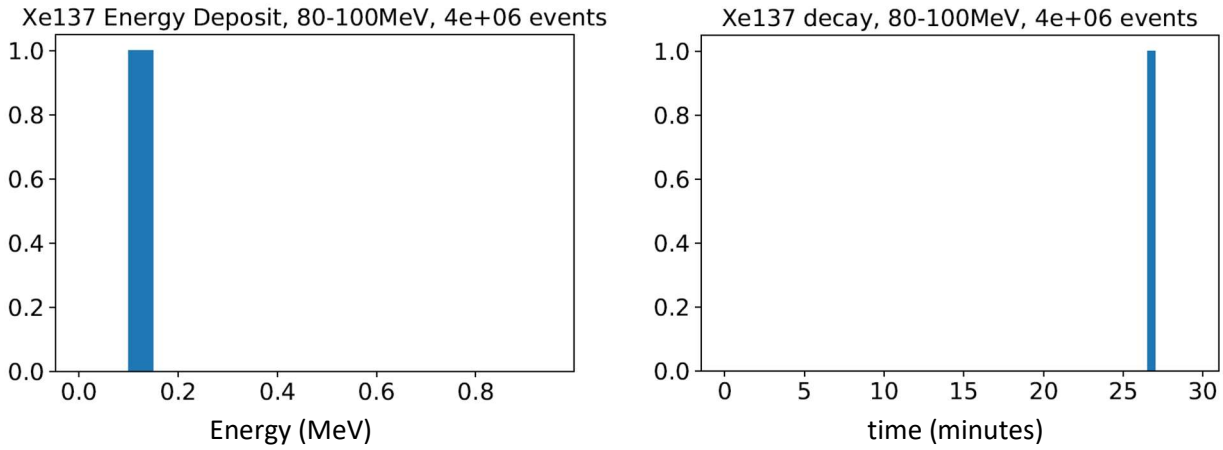

Figure 23. The above histograms display the deposited energies (LEFT) and the time for radioactive decay (RIGHT) for created ^{137}Xe for events at 80-100 MeV.

Figure 24 shows the creation of one ^{64}Cu isotope per 172 years, one ^{66}Cu per 400 years, and no ^{137}Xe due to cosmogenic neutrons. Associated energy deposits and decay times are shown below in Figures 26 and 27.

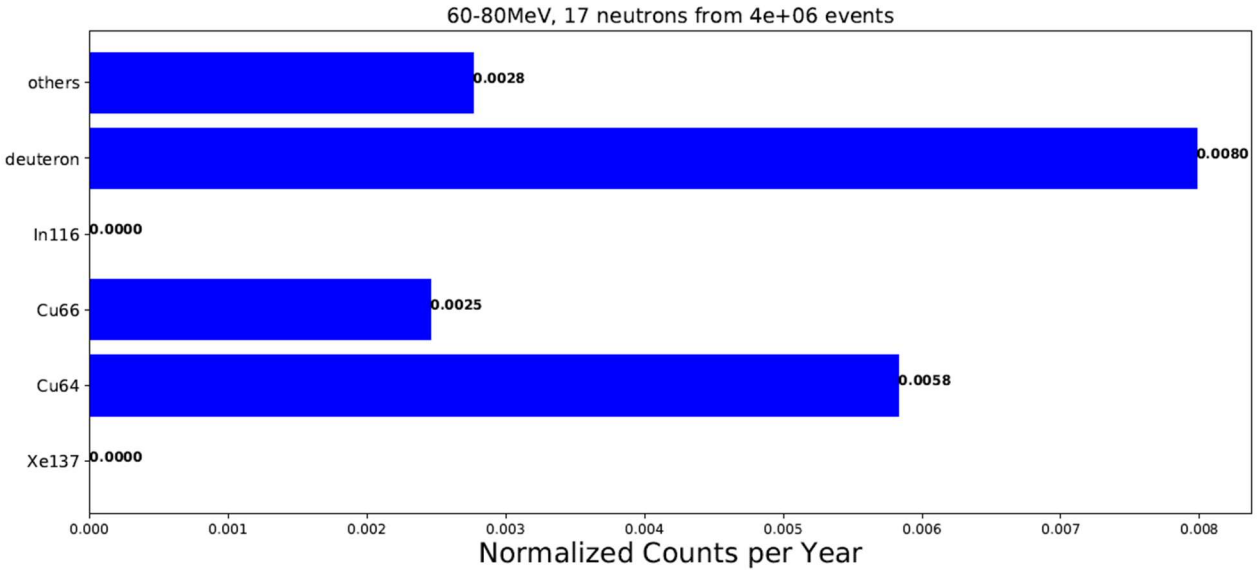

Figure 24. The figure above displays the normalized counts of isotopes of interest within the detector. These are resultant from 17 neutron captures out of 4 million neutrons generated at 60-80 MeV.

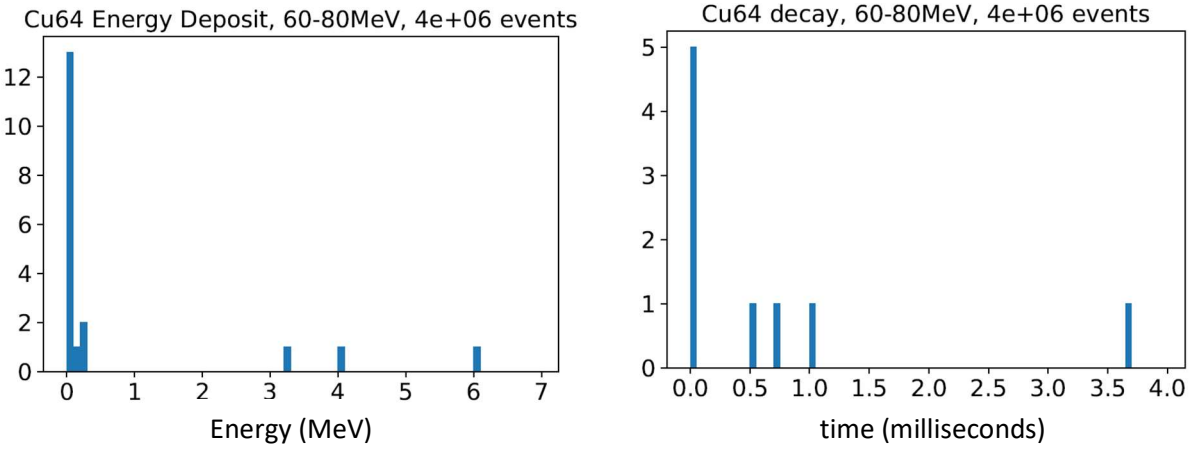

Figure 25. The above histograms display the deposited energies (LEFT) and the time for radioactive decay (RIGHT) for created ^{64}Cu for events at 60-80 MeV.

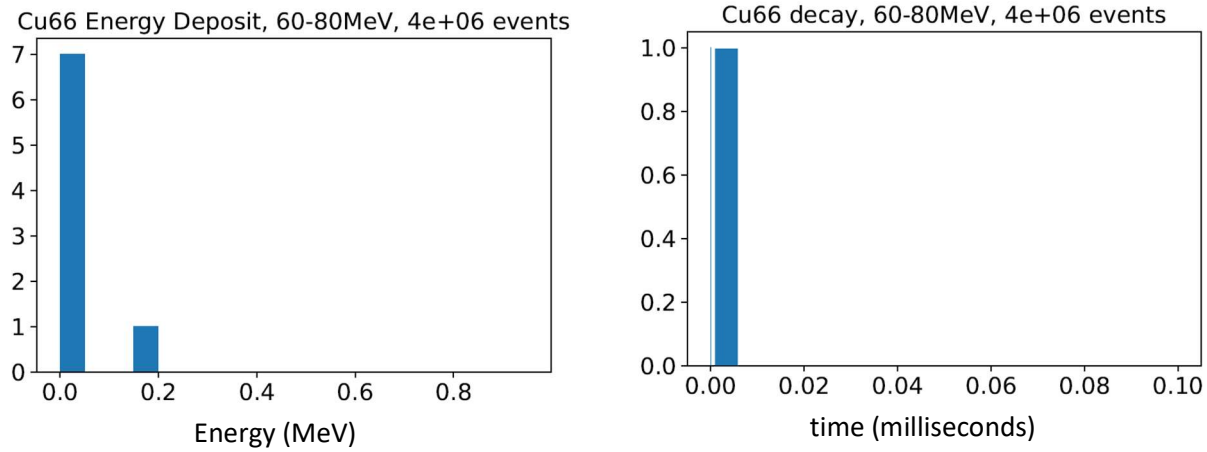

Figure 26. The above histograms display the deposited energies (LEFT) and the time for radioactive decay (RIGHT) for created ^{66}Cu for events at 60-80MeV.

Figure 27 shows the creation of one ^{64}Cu isotope per 96 years, no ^{66}Cu, and no ^{137}Xe due to cosmogenic neutrons. There are no significant associated energy deposits or decay times for this energy range.

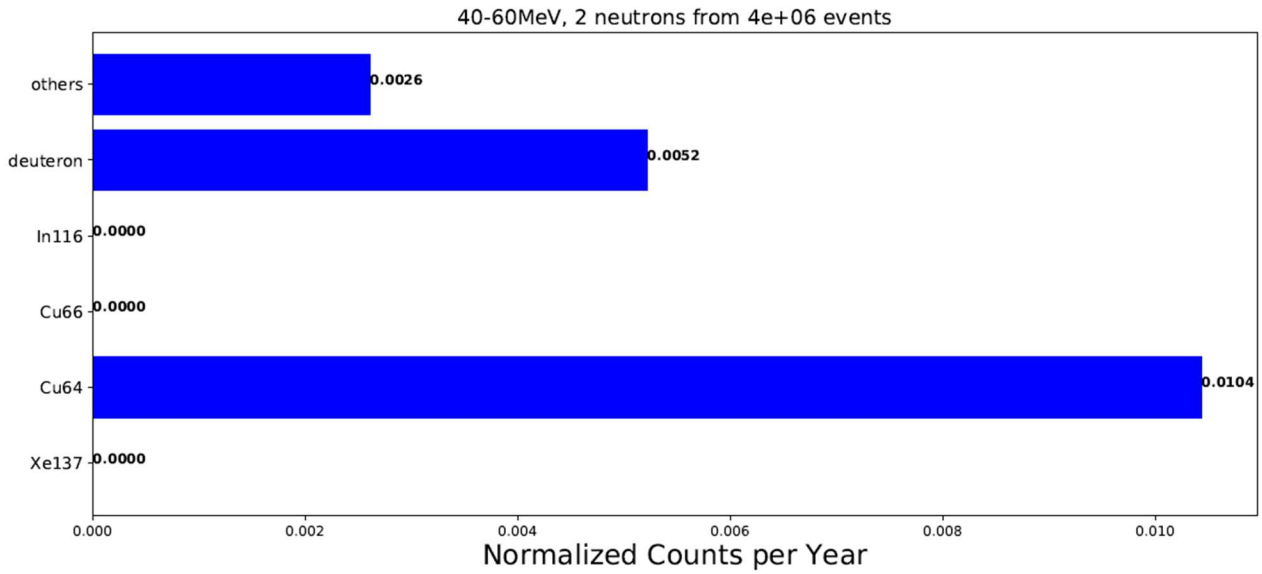

Figure 27. The figure above displays the normalized counts of isotopes of interest within the detector. These are resultant from 2 neutron captures out of 4 million neutrons generated at 40-60 MeV.

- **MUON GENERATION**

Results for simulation of cosmogenic muons are still in the preliminary phase an require further investigation. The energy range of muons is expected to be within that for existing labs; however,

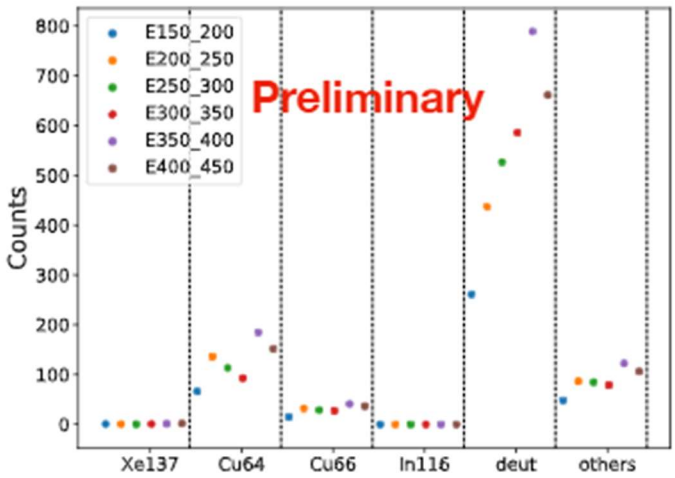

Figure 28. Preliminary expected isotopic generation from cosmogenic muons simulated at energies 150 – 450 MeV, created by REST member Leslie Rogers.

the full statistics are yet to be analyzed. Generation of muons presents a much heavier computational burden than neutrons. Therefore, generating high enough counts to produce significant results takes a much longer time and drain on the shared server in which the simulations are done.

3.4 DISCUSSION OF COSMOGENIC SIMULATIONS

Simulations of neutrons generated from a plane outside the tonne-scale detector have shown improvement over previous designs in reduction of neutrons interactions. We find that neutron captures within the detector occur more frequently for higher energy neutrons. Neutron generation at energy range 60-80 MeV resulted in 17 neutron captures and 2 neutron captures 40-60 MeV per 4 million neutrons. Our study observes that cosmogenic neutrons below energy 40 MeV create no significant isotopes nor leave energy deposits that may interfere with this experiment.

For neutrons at 80-100 MeV, we observe 79 neutron captures and one ^{137}Xe activation for every 4 million neutrons. This shows an energy deposition less than 0.2 MeV and a decay occurring between 25 and 30 minutes. The bulk of isotopic generation appears to occur in the copper shielding with the production of ^{64}Cu and ^{66}Cu. Energy deposits are expected as high as 12 MeV but generally fall below 6 MeV with the majority below 1 MeV and should have no overall effect on the experiment. No ^{137}Xe activations are seen from neutrons below 80 MeV.

We observe an overall low level of ^{137}Xe contributions via muons events, though further study is necessary to determine ^{137}Xe sensitivity. Additionally, an increasing count of other isotopes with increasing muon energy with a large contribution of deuterium for reasons not yet understood (see Figure 20).

4. CONCLUSION

Developing a viable control in argon gas that displays time constant of ≈ 3.1 μs has proven non-trivial and requires extensive testing. We have developed a prefatory understanding of how our system behaves and how data must be analyzed. This will serve as the basis for our continued systematic study of pure and, eventually, doped argon scintillation at various pressures. We will continue to experiment with the effects of TPB which may improve our result. It is also of interest to develop a better understanding of applying an electric field and electroluminescent qualities within the chamber.

We find that the scaling of the NEXT detector to a tonne-scale design, with the replacement of a polyethylene shield with a water tank, shows significant improvement. We conclude that the water tank is effective in the reduction of cosmogenic neutrons and that their background contribution is essentially negligible. Although, we may continue this study by testing the effects of doping the water tank with other neutron capturing molecules that may improve our results further. Overall, the continued focus of this study will be on the generation and effects of muons. Newly developed analysis code will allow for better energy spectra and understanding of rejection factors at various muon energies. It will also allow for the variation of energy with respect to the depth of the detector.

Neutrino experiments are engaged in a constant push for finer sensitivity to explore more elusive, non-standard-model effects. It is tests like these that may discover interesting or unexpected results that may impact large-scale experiments. This study conveys the importance of small-scale and simulated demonstrations for further development in experimentation.

5. ACKNOWLEDGEMENTS

This research was funded by the UTA College of Science as well as the National Science Foundation Grant P217A180234 in conjunction with the University of Texas at Arlington McNair Scholars Program. Special thanks to the members of the UTA Rare Event Searches and Techniques team, Dr. David Nygren and the NEXT Collaboration, the IFIC at the University of Valencia, and notable mention to Dr. Joan Reinhardt, Natalie Stephens, and Cheri Counts for their assistance and guidance.

6. REFERENCES

[1] J. Munoz Vidal, Ph.D. in Physics, *The NEXT path to inverse neutrino hierarchy,* Universitat de Valencia (2018)

[2] NEXT Collaboration, V. Alvarez, et al., *The NEXT-100 experiment for 0νββ searches at LSC*, JINST **7**. (2011) [arXiv: 1106.3630]

[3] NEXT Collaboration, V. Alvarez, et al**.,** *Ionization and scintillation response of high-pressure xenon gas to alpha particles,* JINST **8**. (2013) [arXiv:1121.4508]

[4] DUNE Collaboration, R. Acciarri, et al., *Long-Baseline Neutrino Facility (LBNF) and Deep Underground Neutrino Experiment: Conceptual Design Report,* The DUNE Detectors at LBNF **4**. (2016) [arXiv: 1601.20984]

[5] C. Amsler, V. Boccone, A. Buchler, R. Chandrasekharan, C. Regenfus, J. Rochet, *Luminescence quenching of the triplet excimer by air traces in gaseous argon*, JINST **3**. (2008)

[6] R. Acciarri, M. Antonello, B. Baibussinov, M. Baldo-Ceolin, P. Benetti, F. Calaprice, E. Calligarich, M. Cambiaghi, N. Canci, F. Carbonara, F. Cavanna, S. Centro, A.G. Cocco, F. Di Pompeo, G. Fiorillo, C. Galbiati, V. Gallo, L. Grandi, G. Meng, I. Modena, C. Montanari, O. Palamara, L. Pandola, F. Pietropaolo, G.L. Raselli, M. Roncadelli, M. Rossella, C. Rubbia, E.

Segreto, A.M. Szelc, S. Ventura, and C.Vignoli, *Effects of Nitrogen contamination in liquid Argon*, JINST **5**. (2010) [arXiv: 0804.1217]

[7] Y. Nakajima, A. Goldschmidt, H.S. Matis, D. Nygren, C Oliveira, and J. Renner, *Measurement of scintillation and ionization yield with high-pressure gaseous mixtures of Xe and TMA for improved neutrinoless double beta decay and dark matter searches,* JINST **11**. (2016) [arXiv: 1505.03585]

[8] Y. Nakajima, A. Goldschmidt, M. Long, D. Nygren, C Oliveira, and J. Renner, *Micro-physics simulations of columnar recombination along nuclear recoil tracks in high-pressure xe gas for directional dark matter searches*, J. Phys. Conf. Ser. **650**. (2015)

[9] C.G. Wahl, E.P. Bernard, W.H. Lippincott, J.A. Nikkel, Y. Shin, and D.N. McKinsey *Pulse-shape discrimination and energy resolution of a liquid-argon scinillator,* JINST **9**. (2014) [arXiv: 1403:0525]

[10] *Photomultiplier Tubes: principles and Basics,* 3rd (a) Ed., (Hamamatsu Photonics, 2007)

[11] V.A. Kudryavtsev, L. Pandola, and V. Tomasello, Eur. Phys. J. A **36**. (2008)

[12] W.H. Trzaska, M. Slupecki, I. Bandac, A. Bayo, A. Bettini, L. Bezrukov, T. Enqvist, A. Fazliakhmetov, A. Ianni, L. Inzhechik, J. Joutsenvaara, P. Kuusinimei, K. Loo, B. Lubsandorzhiev, A. Nozik, C. Pena Garay, and M. Poliakova, *Cosmic-ray muon flux at Canfranc Underground Laboratory,* Eur. Phys. J. (2019) [arXiv: 1902.00868]

[13] Geant4 Collaboration, S. Agostinelli et al., Geant4: A simulation toolkit, Nucl. Instrum. Meth. A **506** (2003) 250–303. Software available online at http://geant4.cern.ch/.